JOURNAL OF SOLID STATE CHEMISTRY **18,** 17–25 (1976)

Physicochemical Properties of Alkali Metal Cation–TCNQ Anion Radical Salts

ICHIMIN SHIROTANI AND NOBUKO SAKAI

The Institute for Solid State Physics, The University of Tokyo, Roppongi, Minato-ku, Tokyo 106

Received October 3, 1974; in revised form December 19, 1975

Simple alkali metal cation–TCNQ anion radical salts are classified in two groups from the differences in their physicochemical properties and crystal structures. Li–, Na–, K–, and Rb(I)–TCNQ are comprised in Group A. Li–TCNQ exhibits distinct behavior from other salts in Group A. Rb(II)– and Cs–TCNQ belong to Group B. Phase transitions, electrical conductivities, and absorption spectra in these simple salts are closely related to their crystal structures.

Introduction

Electrical (*1–3*), optical (*4–6*), and magnetic properties (*7*, *8*), and crystal structures (*9–12*) in simple alkali metal cation–TCNQ anion radical salts (*M*–TCNQ) have been studied. Phase transitions are observed in the temperature range −150 to 300°C (*13*, *14*). The crystal structures of the low- and high-temperature modifications of Na–TCNQ have been recently determined (*15*). Further, new pressure-induced phase transitions have been investigated at room temperature (*14*). Physical properties and crystal structures of *M*–TCNQ depend strongly on the nature of the cation. According to the differences in their physical properties and crystal structures, simple TCNQ salts are classified into two groups. Li–, Na–, K–, and Rb(I)–TCNQ are comprised in Group A. However, Li–TCNQ exhibits somewhat distinct behavior from other salts in Group A. Rb(II)– and Cs–TCNQ belong to Group B.

In a previous paper, we presented some findings on the phase transitions and the electrical and optical properties in *M*–TCNQ (*2–4*, *14*). In this paper the relation between physicochemical properties and crystal structures in these salts will be discussed.

Crystal Structures

X-ray studies of TCNQ salts have revealed that the TCNQ molecules are stacked face to face to form columns in most of these crystal structures. The infinite columns hitherto reported consist of tetradic, triadic, diadic, and monadic units of TCNQ molecules. The columnar structures of TCNQ salts seem to be closely related to electrical conductivity (*16*). The TCNQ salts with diadic, triadic, and tetradic units are low or intermediately conductive. The highly conductive salts such as TTF–TCNQ are constructed of monadic units of TCNQ. Crystal structures of several *M*–TCNQ have already been determined (*9–12*). Crystal data of simple salts are summarized in Table I. The columnar structures of Na–, K–, and Rb(I)–TCNQ salts consist of diadic units of $TCNQ^-$. On the contrary, in the case of Rb(II)–TCNQ salt, the columns constructed from monadic unit of $TCNQ^-$ are found. Figure 1 shows the mode of overlapping between nearest $TCNQ^-$ in Rb(I)– and Rb(II)–TCNQ salts. The nearest neighbor overlap of $TCNQ^-$ in Na– and K–TCNQ is similar to that in Rb(I)–TCNQ. The overlapping mode of Rb(II)–TCNQ resembles that of high conductive salt such as

TABLE 1

CRYSTAL DATA OF M–TCNQ

Compound	Crystal data		Mode of nearest neighbor overlap of TCNQ$^-$	Periodic unit of TCNQ$^-$
Li–TCNQ	Tetragonal	$a = b = 12.3$ $c = 7.9$ $z = 4$		
Na–TCNQ	$C\bar{1}$	$a = 6.993$ $b = 23.707$ $c = 12.469$ $\alpha = 90.14$ $\beta = 98.58$ $\gamma = 90.76$ $z = 8$	Rb(I) salt type	2
K–TCNQ	$P2_1/n$	$a = 7.10$ $b = 17.80$ $c = 17.88$ $\beta = 94.9$ $z = 8$	Rb(I) salt type	2
Rb(I)–TCNQ	$P2_1/c$	$a = 7.187$ $b = 12.347$ $c = 13.081$ $\beta = 98.88$ $z = 4$ at −160°C	Rb(I) salt type	2
Rb(II)–TCNQ	$P\bar{1}$	$a = 9.914$ $b = 7.196$ $c = 3.903$ $\alpha = 92.70$ $\beta = 86.22$ $\gamma = 97.73$ $z = 1$	Rb(II) salt type	1

TTF–TCNQ. The remarkable differences of the crystal structures of both Rb salts are illustrated in Figs. 2 and 3.

Within the columns of Rb(I) salt, the dimerized structure of TCNQ$^-$ appears, interplanar spacing of 3.159 and 3.484 Å alternating *(10)*, whereas in the case of Rb(II) salt, all TCNQ$^-$ ions in column are equivalent, the interplanar spacing being 3.43 Å *(11)*.

The crystal structures of Na– and K–TCNQ are similar to those of Rb(I)–TCNQ. The structure of Cs–TCNQ has not yet been determined. Judging from the physicochemical properties of Cs–TCNQ, its structure seems to resemble that of Rb(II)–TCNQ.

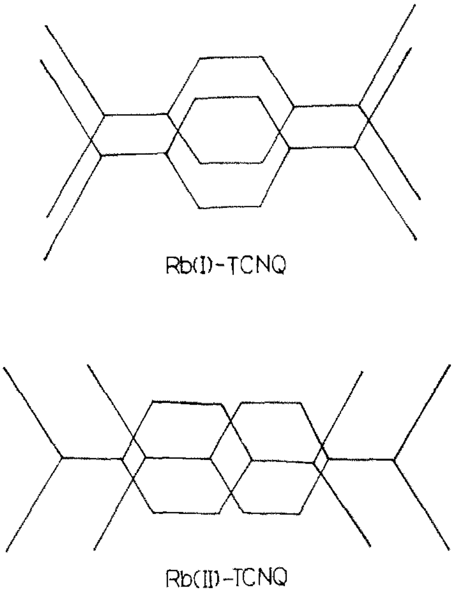

FIG. 1. Nearest neighbor overlap of TCNQ anion for Rb salts.

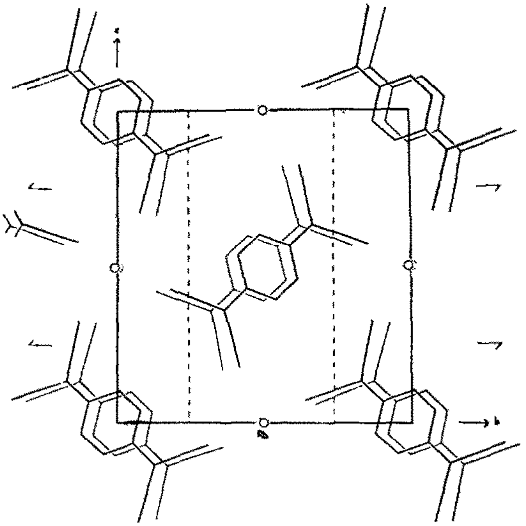

FIG. 2. Projection of the structure along the a-axis in Rb(I)–TCNQ.

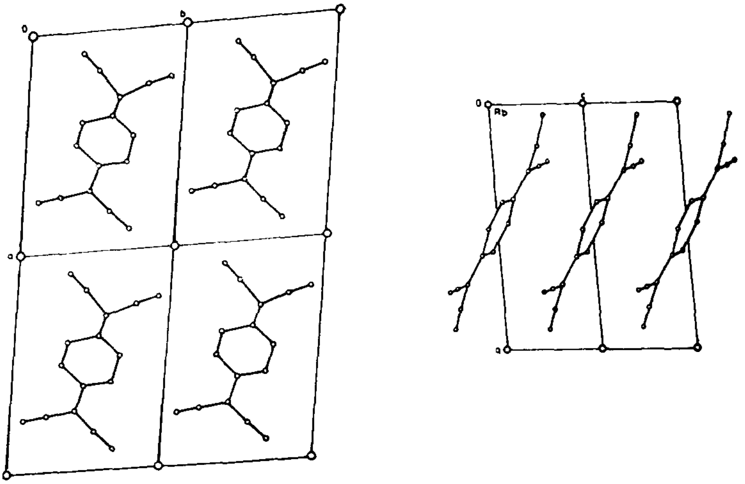

FIG. 3. Projection of the structure along the *c*-axis and *b*-axis in Rb(II)–TCNQ.

Phase Transitions at Atmospheric Pressure

Phase transitions in *M*–TCNQ have been observed in the temperature range −150 to +300°C; the transition temperature of Group A is above room temperature and that of Group B is below 0°C. At room temperature, Na–, K–, and Rb(I)–TCNQ belong to the low-temperature phase and Rb(II)– and Cs–TCNQ belong to the high-temperature phase. The phase transition in Li–TCNQ is not observed at atmospheric pressure. These results are summarized in Table II.

Recently, the crystal structures of the low- and high-temperature modifications of Na–TCNQ have been determined (*15*). Crystal data of the low temperature are shown in Table I. The $TCNQ^-$ anions form a columnar structure along the *a*-axis with alternating interplanar distances of 3.21 and 3.49 Å. $TCNQ^-$ dimers are recognized in the structure. The crystals of the high temperature phase are monoclinic with space group $P2_1/n$ and lattice constants: $a = 3.512$, $b = 11.806$, $c = 12.465$ Å, $\beta = 98.21$, and $z = 2$. $TCNQ^-$ ions are stacked face to face to form

TABLE II

TRANSITION TEMPERATURE, HEAT OF TRANSITION ΔH, AND ELECTRICAL ANOMALIES AT HIGH PRESSURE FOR SIMPLE TCNQ SALTS

Compounds	Transition temperature (°K)		Heat of transition[a] ΔH (cal/mole)	Electrical anomalies[b] at high pressure (kbar)
Li–TCNQ	No phase transition observed			8.5
Na–TCNQ	338[b]	348[a]	Unobservable	1.5, 6, 12
K–TCNQ	391	395	60	2, 6, 10
Rb(I)–TCNQ	374	381	1010	1, 3.5
Rb(II)–TCNQ	231	223	—	No anomalies observed
Cs–TCNQ	254	210	Unobservable	No anomalies observed

[a] Ref. (*13*).

[b] Ref. (*14*).

columns along the *a*-axis with an equal interplanar spacing of 3.385 Å. The structure is composed of monomeric $TCNQ^-$ and Na^+. The dimeric structure transforms into monomeric above the transition temperature (T_c). The monomer–dimer transition (M–D transition) is a common nature of *M*–TCNQ (*17*).

The slope obtained from the pressure–temperature phase diagram of Rb(I)–TCNQ is

$$dP/dT = +0.36 \text{ kbar/degree}. \qquad (1)$$

The discontinuity in volume at the transition point is calculated from the Clapeyron–Clausius relation for the first-order phase transition

$$dP/dT = \Delta S/\Delta V, \qquad (2)$$

where ΔS is an entropy change between two phases. ΔS for this salt, evaluated from a heat of transition, is about 2.65 cal/mole. Consequently, ΔV is 0.31 cm^3/mole. The phase separation line in Na–TCNQ is approximately linear with a slope, dP/dT, of +0.014 kbar/degree.

It is well known that Würster's Blue Perchlorate (WBP) shows an orthorhombic → monoclinic phase transition at 186°K. Then, in the low-temperature phase, WB cations pair up to form dimers in the column. The dP/dT of this compound is +0.1 kbar/degree (*18*). It should be noted that the dP/dT of the M–D transitions in ion radical salts is positive.

Recently, we investigated the X-ray critical scattering near T_c in such crystals as Na–TCNQ and WBP (*19*). The temperature dependences of the scattering intensity of the (1.5, $\bar{1}$, 0) reflection in Na–TCNQ and the (3.5, 0, 0.5) reflection in WBP have been studied. These superlattice reflections appearing below T_c are most sensitive to the motion of $TCNQ^-$ or WB^+. The intensity of these reflections decreases with increasing temperature and drops abruptly at T_c. The measurements of diffuse intensity around the above reciprocal points have been carried out. The intensity increases rapidly on approaching T_c. The temperature dependences of these intensities are explained by the behavior of the soft phonon.

New Pressure-Induced Phase Transition

Figure 4 shows the pressure–resistance curve at room temperature for polycrystalline Li–TCNQ. The resistance decreases to about 5 kbar, and then it increases, attaining its maximum at about 8.5 kbar, and then

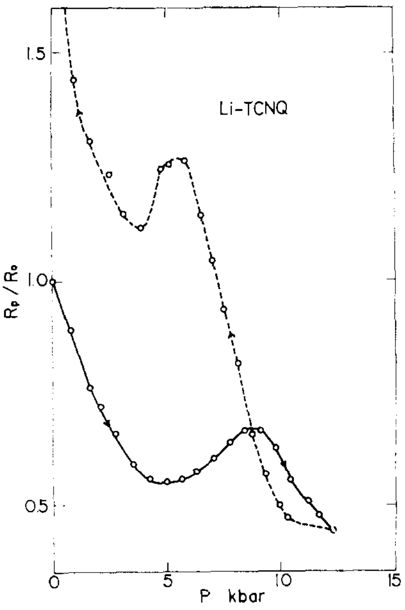

FIG. 4. Relative resistance as a function of the pressure in the pellet of polycrystalline Li–TCNQ.

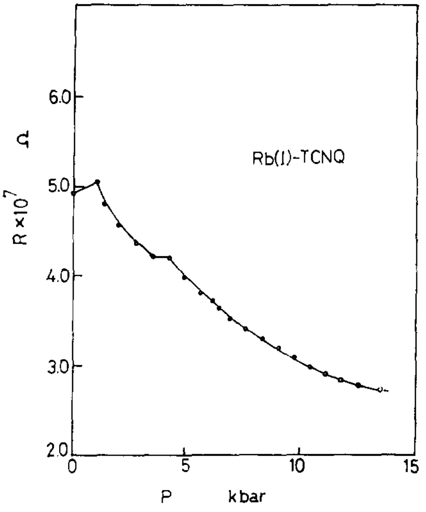

FIG. 5. The effect of pressure on the resistivity in Rb(I)–TCNQ single crystal.

decreasing again. Though no phase transition at atmospheric pressure has been observed over the wide temperature range, the anomaly in the electrical resistance at high pressure arises from the new pressure-induced phase transition. The effect of pressure on the resistivity in Rb(I)–TCNQ is illustrated in Fig. 5. The anomalies in the resistivity are found at about 1 and 3.5 kbar. This may be due to the appearance of the new phase at high pressure since dP/dT for temperature phase at 1 bar is positive. The nature of new phase transitions in M–TCNQ is not well known.

The anomalous electrical behavior at high pressure is observed in TCNQ salts of Group A. On the contrary, the resistivity of Group B decreases monotonously at least up to 13 kbar.

Crystal Chemistry

The crystal structures and phase transitions of AX compounds, which is essentially an ionic bond, are related to the ionic radius ratio r^+/r^-. In the case of M–TCNQ the chemical bond is very complex. The intermolecular forces in these salts contain mainly the Coulomb forces between alkali cation and TCNQ anion, van der Waals and the charge transfer forces among $TCNQ^-$ anions. The magnitude of the intermolecular energy is estimated by Kobayashi (*20*); the Madelung energy for K–TCNQ is about 83 kcal/mole, the charge transfer energy being several kilocalories per mole, the van der Waals energy being about 20 kcal/mole. Therefore, a slight change of the external condition may induce the instability of the crystal lattice in ion radical salts because of the complicated molecular interaction in them. The many phase transitions over wide temperature and pressures ranges arise from the complex intermolecular interaction.

The crystal structures and the physical properties of TCNQ salts depend on the nature of the cation. The electronic polarizability of cation, which is related to the ionic radius, is an important determinant of the variation in the physical properties (*21*). The ionic radii of Li^+, Na^+, K^+, Rb^+, and Cs^+ are 0.78, 0.98, 1.33, 1.49, and 1.69 Å, respectively. The polarizing powers, which are equal to Ze/r^2 (Z, number of charge; e, elementary charge; r, ionic radius), are 1.64, 1.04, 0.57, 0.45, and 0.34 (arbitrary unit) for Li^+, Na^+, K^+, Rb^+, and Cs^+, respectively. The effect of this power cannot be ignored for a molecule with π electrons. If the polarizing power of M^+ is large, the columnar structures in M–TCNQ consist of the diadic units of $TCNQ^-$. Similar results have been observed for alkali metal–chloranil salts (M–CA) (*22*). The chloranil anions (CA^-) associate bimolecularly in the crystalline state in Li– and Na–CA. The absorption spectra of K– and Rb–CA show the nature of the monomer in the crystalline state (*23*). Since dP/dT of M–D transition is positive, the volume of the high-temperature phase is larger than that of the low-temperature phase. The structures of the high-temperature phase in M–TCNQ are constructed of monomeric $TCNQ^-$. This may arise from the decrease of polarizing power with increasing the volume.

The behavior of simple salts with smaller ionic radius is different from that of the TCNQ salts with larger ionic radius. Rb–TCNQ is the compound located on the boundary region. Therefore, this salt is polymorphic at room temperature. In the case of the large cation such as Cs^+, the component ratio between the donor and the acceptor is possible to change, forming the complex salt, Cs_2–$TCNQ_3$.

Electrical Properties

Table III shows the electrical properties of simple TCNQ salts. Their electrical resistivity exhibits a semiconductive behavior; $\rho \simeq 10^4$ to 10^5 Ω cm with activation energy $\Delta E = 0.3 \sim 0.4$ eV for TCNQ salts in Group A and $\rho \simeq 10^2$ Ω cm with activation energy $\Delta E = 0.16 \sim 0.2$ eV for Group B. The electrical resistances of M–TCNQ decrease rapidly with increasing pressure up to 135 ~ 170 kbar. The least resistivities for Group A are about 0.2 ~ 3 Ω cm and for Group B are about 0.06 ~ 0.1 Ω cm. Li–TCNQ exhibits distinct behavior from other salts in Group A at high pressure.

Columnar structures of TCNQ salts seem to be closely related to the electrical con-

TABLE III

THE ELECTRICAL PROPERTIES FOR SIMPLE TCNQ SALTS

	Single crystal[a]		Microcrystal[b]		Minimum resistivity at high pressure[c,d] (Ω cm)
	Resistivity (Ω cm)	Activation energy (eV)	Resistivity (Ω cm)	Activation energy (eV)	
Li–TCNQ			5×10^5	0.32	$\sim 2 \times 10^{-1}$ (135 kbar)
Na–TCNQ	$\sim 1 \times 10^3$ (‖) $\sim 5 \times 10^4$ (⊥)	$0.23 \sim 0.32$	1×10^5	0.33	$\sim 3 \times 10^0$ (174 kbar)
K–TCNQ	$\sim 5 \times 10^3$ (‖) $\sim 2 \times 10^5$ (⊥)	$0.15 \sim 0.45$	1×10^4	0.35	$\sim 3 \times 10^0$ (148 kbar)
Rb(I)–TCNQ	$\sim 3 \times 10^5$ (‖) $\sim 3 \times 10^6$ (⊥)	$0.44 \sim 0.53$			$\sim 1 \times 10^0$ (135 kbar)
Rb(II)–TCNQ	$\sim 1 \times 10^2$ (‖)	$0.16 \sim 0.22$			$\sim 6 \times 10^{-2}$ (170 kbar)
Cs–TCNQ	$\sim 6 \times 10^2$ (‖)	~ 0.16	3×10^3	0.18	$\sim 1 \times 10^{-1}$ (152 kbar)

[a] Ref. (*2*).

[b] Ref. (*1*).

[c] Ref. (*3*).

[d] The electrical resistance of *M*–TCNQ decreases rapidly with increasing pressure and reaches the minimum in the pressure range 135 ~ 175 kbar. Above these pressures the solid phase reaction is induced by applied pressure. (‖) along the needle axes; (⊥) perpendicular to needle axes.

ductivity (*16*). The TCNQ salts with diadic, triadic, and tetradic units are low or intermediately conductive. The high conductive salts such as qinolinium–TCNQ$_2$ (Q–TCNQ$_2$), *N*-methylphenazinium–TCNQ (NMP–TCNQ), and TTF–TCNQ are constructed of monadic units of TCNQ. The crystals of Rb(I)–TCNQ in Group A have monoclinic symmetry and TCNQ$^-$ ions are stacked face to face to form columns of diadic units of TCNQ$^-$. On the contrary, in the case of the Rb(II) salt, all TCNQ$^-$ anions in the column are equivalent. As is shown in Table III, the resistivities of Group A are about 10^3 times more than those of Group B. This arises from the difference of the columnar structure.

The conductivities of TCNQ salts depend strongly on the nature of the cation. The electronic polarizability of the cation is an important determinant of the variation in the conductivity (*21*). Heterocyclic aromatic cations in high conductive TCNQ salts have large polarizability, while atomic cations are very small. The columnar structure of Rb(II)–TCNQ is very similar to that found in the crystals of NMP–TCNQ though interplanar spacing between TCNQ$^-$ is different. The electrical conductivities in the high conductive TCNQ salts are 10^4 times more than those in Rb(II) salt. This difference is mainly explained by the magnitude of the cation polarizability.

Peierls showed (*24*) that within the limit of one electron theory the one-dimensional metallic state becomes unstable owing to the presence of the periodic potential, and thus, the linear electron system must be an insulator. The dimerized structure in the TCNQ columns appears to be typical for simple *M*–TCNQ; these salts exhibit the semiconductive behavior. In the case of Rb(II)–TCNQ, all the TCNQ$^-$ ions in the column are equivalent. This columnar structure resembles that found in the crystals of NMP–TCNQ. Magnetic susceptibility and conductivity measurements for NMP–TCNQ indicate a metallic state above 200°K with a continuous transition to an insulator below 200°K (*25*). However, insulator–metal transition for Rb(II)–TCNQ

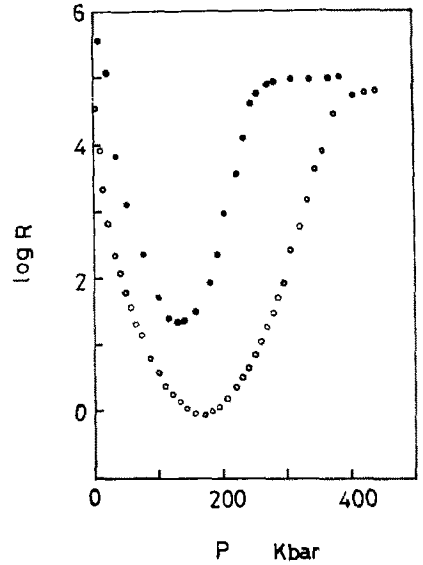

FIG. 6. The effect of pressure on the resistance of compacted specimen in Rb–TCNQ. ●, Rb(I) salt; ○, Rb(II) salt.

has not been observed in the wide temperature range 170 to 570°K. Since the interplanar spacing between TCNQ$^-$ anion in Rb(II) salt, 3.43 Å, is much longer than that in NMP–TCNQ, 3.26 Å, the band model seems to give a poor description for Rb(II)–TCNQ.

Figure 6 exhibits the effect of pressure on the resistance of compacted specimen for Rb(I) and Rb(II) salts. Their electrical resistances decrease rapidly with an increase in the pressure and reach their minimum at pressure of 135 or 170 kbar. The least resistivities of *M*–TCNQ are given in Table III. These values for Group A are about 0.2 ~ 3 Ω cm and for Group B are about 0.06 ~ 0.1 Ω cm. Above 135 or 170 kbar, the electrical resistances of Rb salts increase rapidly with the increase in the pressure. This behavior arises from the pressure-induced solid phase reaction (*3*). The minimum pressures at which the reaction is induced are given in Table III. It should be noted that for Group B this pressure is larger than for Group A except in the case of Na–TCNQ. The differences of the minimum resistivities and reactivity at high pressure between Groups A and B have been explained by the differences of their columnar structures.

Optical Properties

Figure 7 shows the absorption spectra of Rb(I)- and Rb(II)–TCNQ. The absorption bands in the visible region are locally excited (LE) bands within the TCNQ$^-$ anion. These bands exhibit the spectral blue shift with pressure. The rate of pressure shift is given in Table IV. The near-infrared band observed in Rb salts is assigned to the charge transfer (CT) band between TCNQ$^-$ anion. The pressure effect on the CT band could not be observed because of interference by the pressure-transmitting fluid. However, CT band may be expected to be shifted to the longer wavelength region with pressure.

From the differences in the transition energy and the oscillator strength, alkali metal cation–TCNQ salts have already been classified into two groups (*6*). Though the transition energies of the LE bands in Groups A and B are almost the same, the pressure shifts of Group B are larger than those of Group A. Further, CT bands of Group B shift toward longer wavelength than those of Group A. These results are summarized in Table IV.

In a previous paper, we reported (*22*) that the absorption spectra of Li- and Na–CA show the striking difference compared with those of K- and Rb–CA. The solid-state spectra of Li- and Na–CA are similar to those of the dimer [(CA$^-$)$_2$] in a solution, whereas the spectra of K- and Rb–CA resemble those of the monomer (CA$^-$) in solution. The chloranil anion radical seems

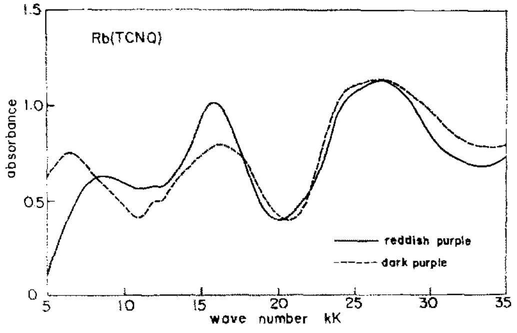

FIG. 7. The absorption spectra of Rb–TCNQ. Reddish purple, Rb(I) salt; dark purple, Rb(II) salt.

TABLE IV

TRANSITION ENERGY AND RATE OF PRESSURE SHIFT FOR SIMPLE TCNQ SALTS

	LE band kH	Rate of pressure Shift (cm^{-1}/kbar)	CT band kH
Li–TCNQ	26.5	+86	8.0
	16.0	+51	
Na–TCNQ	27.5	+49	8.3
	16.1	+47	
K–TCNQ	26.2	+58	8.3
	16.1	+45	
Rb(I)–TCNQ	26.4	—	8.6
	16.1	—	
Rb(II)–TCNQ	26.2	+67	6.5
	16.1	+62	
Cs–TCNQ	25.9	—	6.5
	15.7	+62	

to be in the dimeric for the former and to be in the monomeric for the latter in the crystal. Therefore, in the case of simple M–TCNQ, the differences of optical properties arise from those of the columnar structures.

Acknowledgments

The authors would like to thank Prof. H. Inokuchi for useful suggestions and Prof. S. Minomura for his encouragement in the work. Their thanks are also due to Drs. H. Kobayashi, Y. Ohashi, and A. Onodera for helpful discussion.

References

1. W. J. SIMONS, P. E. BIERSTEDT, AND R. G. KEPLER, *J. Chem. Phys.* **39**, 3523 (1963); R. G. KEPLER, *J. Chem. Phys.* **39**, 3528 (1963).
2. N. SAKAI, I. SHIROTANI, AND S. MINOMURA, *Bull. Chem. Soc. Japan* **45**, 3316 (1972).
3. I. SHIROTANI, A. ONODERA, AND N. SAKAI, *Bull. Chem. Soc. Japan* **48**, 167 (1975).
4. I. SHIROTANI, N. SAKAI, H. INOKUCHI, AND S. MINOMURA, *Bull. Chem. Soc. Japan* **42**, 2087 (1969); N. SAKAI, I. SHIROTANI, AND S. MINOMURA, *Bull. Chem. Soc. Japan* **43**, 57 (1970).
5. Y. IIDA, *Bull. Chem. Soc. Japan* **42**, 71 (1969).
6. Y. OHASHI AND T. SAKATA, *Bull. Chem. Soc. Japan* **46**, 3330 (1973).
7. R. G. KEPLER, *J. Chem. Phys.* **39**, 3528 (1963).
8. J. G. VEGTER AND J. KOMMANDEUR, *Phys. Rev.* **B7**, 2929 (1973).
9. G. R. ANDERSON AND C. J. FRITCHIE, JR., Paper for Second National Meeting of the Society for Applied Spectroscopy, San Diego (1963).
10. A. HOEKSTRA, T. SOPIEDER, AND A. VOS, *Acta Crystallogr.* **B28**, 14 (1972).
11. I. SHIROTANI AND H. KOBAYASHI, *Bull. Chem. Soc. Japan* **46**, 2595 (1973).
12. M. KONNO AND Y. SAITO, *Acta Crystallogr.* **B30**, 1294 (1974).
13. J. G. VEGTER, J. HIDMA, AND J. KOMMANDEUR, *Chem. Phys. Lett.* **3**, 427 (1969).
14. N. SAKAI, I. SHIROTANI, AND S. MINOMURA, *Bull. Chem. Soc. Japan* **45**, 3321 (1972).
15. M. KONNO AND Y. SAITO, *Acta Crystallogr.* **B31**, 2007 (1975).
16. H. KOBAYASHI, *Bull. Chem. Soc. Japan* **47**, 1346 (1974).
17. H. KOBAYASHI AND M. KONNO, private communication.
18. D. D. THOMAS, H. KELLER, AND H. M. MCCONNELL, *J. Chem. Phys.* **39**, 2321 (1963); R. C. HUGHES, A. W. MERKEL, AND H. M. MCCONNELL, *J. Chem. Phys.* **44**, 1720 (1966).

19. H. Terauchi, N. Sakamoto, and I. Shirotani, *J. Chem. Phys.* **64**, 437 (1976).

20. H. Kobayashi and Y. Saito, *Bussei* **11**, 527 (1970).

21. O. H. LeBlanc, *J. Chem. Phys.* **42**, 4307 (1965).

22. N. Sakai, I. Shirotani, and S. Minomura, *Bull. Chem. Soc. Japan* **44**, 675 (1971).

23. The columnar structure of K-CA consists of the monadic units of CA^- ion. M. Konno, H. Kobayashi, F. Marumo, and Y. Saito, *Bull. Chem. Soc. Japan* **46**, 1987 (1973).

24. R. E. Peierls, "Quantum Theory of Solids," Clarendon Press, Oxford (1955).

25. A. J. Epstein, E. Etemad, A. F. Garito, and A. J. Heeger. *Phys. Rev.* **5B**, 952 (1972).